Journal of King Saud University – Science 34 (2022) 102118

Contents lists available at ScienceDirect

Journal of King Saud University – Science

journal homepage: www.sciencedirect.com

Original article

Comparative study of Pd-based electrocatalysts decorated on hybrid carbon supports towards methanol oxidation

Amar Al-Khawlani [a], Basheer M. Al-Maswari [b], Weimin Chen [a,*], Ahmed Boshaala [c], Mohammad I. Ahmad [d], Abdelkader Zarrouk [e], Ismail K. Warad [f,g], Nabil Al-Zaqri [h,*]

[a] School of Environmental and Chemical Engineering, Shenyang Ligong University, Shenyang 110159, China
[b] Department of Chemistry, Yuvaraja's College, University of Mysore, Mysuru, India
[c] Research Centre, Manchester Salt & Catalysis, Unit C, 88-90 Chorlton Rd, M15 4AN Manchester, United Kingdom
[d] Central Laboratories Unit, Qatar University, Doha P.O. Box 2713, Qatar
[e] Laboratory of Materials, Nanotechnology and Environment, Faculty of Sciences, Mohammed V University in Rabat, P.O. Box. 1014, Rabat, Morocco
[f] Department of Chemistry, AN-Najah National University, P.O. Box 7, Nablus, Palestine
[g] Faculty of Pharmacy, Arab American University, P.O. Box 249, Jenin, Palestine
[h] Department of Chemistry, College of Science, King Saud University, P.O. Box 2455, Riyadh 11451, Saudi Arabia

ARTICLE INFO

Article history:
Received 26 January 2022
Revised 27 March 2022
Accepted 18 May 2022
Available online 23 May 2022

Keywords:
Carbon nanotubes
Carbon black
Graphene nanoplates
Bi-hybrid support
Direct methanol fuel cells

ABSTRACT

One suitable strategy to improve the utilisation and performance of Pd-based catalysts in direct methanol fuel cells (DMFCs) is by combining or blending carbon supports. In this study, Pd nanoparticles (NPs) were decorated on bi-hybrid carbon supports consisting of carbon nanotubes (CNTs), graphene nanoplates (GNPs) and carbon black (XC-72) with varying ratios of CNTs: GNPs, CNTs: XC-72 and XC-72: GNPsthrough microwave-assisted ethylene glycol (EG) reduction. All as-prepared catalysts were characterisedby Transmission Electron Microscope (TEM), X-ray diffraction (XRD) and X-ray photoelectron spectroscopy (XPS), and their electrocatalytic activities towards methanol oxidation reaction (MOR) in alkaline solution were investigated by electrochemical measurements. Results indicated that the use of hybrid supports for catalysts substantially increases the electrochemical surface area, reduces the overpotential to methanol oxidation and improves kinetic performance. These effects can be attributed to the unique structure formed after mixing that allows for complete surface utilisation.Among the bi-hybrid electrocatalysts, Pd/CNT-GNP (1:0.1), Pd/CNT-XC-72(1:0.2) and Pd/XC-72-GNP (1:0.2) catalysts have higher activity and better performance.Particularly, Pd/CNT-GNP (1:0.1) catalyst shows a superior activity and the highest oxidation peak current density towards MOR at 57.34 mA/cm^2.TEM and XRD results show that the catalyst nanoparticles on the bi-hybrid carbon support have good dispersion, are not agglomerated and havea small particle size. Hence, the catalyst exhibits an optimised performance and long stability towards methanol electrooxidation in alkaline media.

1. Introduction

In direct methanol fuel cells (DMFCs), methanol oxidation reaction is the main source for producing electrical current. Further improvement on this processcan be achieved by using an appropriate catalyst and catalyst support. Pd-based electrocatalysts are widely used because the Pd in the alkaline medium increasesthe tolerance for carbon monoxide poisoning and the catalytic activity for methanol oxidation (Calderón Gómez et al., 2016; Liu et al., 2014; Nguyen et al., 2011; Shao, 2011; Wei et al., 2011).

Carbon materials have merits as carbon supports, including low cost, quick reduction of metallic phase, superior acid and basic resistance, stable structure at high temperatures and ease of metallic reduction (Cao et al., 2020; Staykov et al., 2014; Wang et al., 2016). As typical SP^2-hybridised carbon material, carbon nanotubes (CNTs) are lightweight and have high effective specific surface area and excellent electrical conductivity (Chiang and Ciou, 2011; Ning et al., 2019). Nevertheless, pristine CNTs are extremely inert to stabilise or optimise metal particles. although carbon tubes

* Corresponding authors.
E-mail addresses: cwmchem@163.com (W. Chen), nalzaqri@ksu.edu.sa (N. Al-Zaqri).
Peer review under responsibility of King Saud University.

Production and hosting by Elsevier

https://doi.org/10.1016/j.jksus.2022.102118
1018-3647/

can be functionalised to create specific sites on their surface for activation, they are still limited and need further improvement.

Carbon black (CB) was also used as a catalyst support due to its highly conductive and extensive surface area. Many studies were carried out to boost CB's performance as a supporting material. However, this material is susceptible to carbon corrosion, particularly under a tough operating environment, which can result in the separation and aggregation of particulate matter in catalysts (Garba et al., 2020; Zhang et al., 2019; Zhang et al., 2017; Zhou et al., 2020). As a promising electrocatalyst support, graphene has gained attention because of its strong electrical conductivity, unique mechanical properties and enormous specific surface area (Schulze et al., 2020; Ghosh et al., 2013; Yousaf et al., 2019; Liu et al., 2019; Mu et al., 2017; Zhang et al., 2018; Chen et al., 2020; Suzuki et al., 2015; Fan et al., 2015). However, van der Waals force causesgraphene nanoplates to stack and reduces the surface area (Tang et al., 2018). In addition to blocking many of the metal nanoparticles' catalytic sites, the stacking creates a large resistance to molecule transport and thus slows down the catalytic activity. Therefore, the catalytic activity and stabilisation of Pd-based catalysts must be further improved. Among the developed methods, choosing a suitable catalyst support has an important effect on the performance of these catalyst (Carvalho et al., 2017; Wu et al., 2011).

The research and modification of catalyst supports have recently aroused widespread interest. Different carbon materials have been used to create a composite support with a unique spatial structure. In addition, CNTs, graphene, activated carbon and other carbon materials are mixed to build a hybrid carrier. The composite carrier's unique spatial structure allows it to outperform a single carbon carrier in terms of mass transfer, reaction rate and catalyst poisoning. Thus, finding effective carbon supports that interact well with metal nanocatalysts is critical (Lv et al., 2021). CNTs and CBwere used to construct hybrid carrier materials and showed good results because the formed unique spatial structure is suitable for loading nano-metal catalyst particles (Gharibi et al., 2010).

Li and co-workers (Li et al., 2012) prepared Pt-based hybrid support catalyst by mixing (XC-72)with reduced graphite oxide (RGO) for oxygen reduction reaction (ORR). In addition to catalytic activity, the composite construction of hybrid support also improved the catalyst's durability; the mixture of (XC-72) between graphene nanoplates resulted in major mass transport in the layer of catalyst and the disturbance of the graphene nanoplates' horizontal stacking (Daş et al., 2019). Additionally, the combination of graphite sheets and CNTs showed novel support with unique properties, and the catalysts exhibited high catalytic activity towards alcohol oxidation (Pham et al., 2016; Fu et al., 2018; Çög enli et al., 2019). Chen and co-workers (Chen et al., 2017) employed graphite nanoplates with CNTs functionalised by chitosan tosynthesise a Pd-based hybrid support catalyst thathas a large active electrochemical surface area (ECSA), a high catalytic activity, and superior resistance to poisoning. These features are attributed to the CNTs mixing with graphene nanoplates in the hybrid support and thus preventing the stacking of graphene nanosheets and enabling the full use of the support surface.

As an extension of our efforts in developing complexes with different types of metal ion center and then converting these complexes into nano-sized materials for catalytic or medical purposes (Warad et al., 2013; Badran et al., 2021; Al-Zaqri et al., 2020; Saleemh et al., 2017; Warad et al., 2014), As in this work, Pd/CNTs-GNPs, Pd/CNTs-XC-72, and Pd/XC-72-GNPs hybrid catalysts with various ratios were synthesised through microwave-assisted reduction with ethylene glycol (EG) as the reducing agent. The prepared electrocatalysts were characterised by TEM, XRD and XPS analysis. Methanol electrooxidation was studied using cyclic voltammetry (CV), linear sweep voltammetry (LSV), chronoamperometry (CA) and electrochemical impedance spectroscopy (EIS). Catalytic activity towards methanol electrooxidationin the alkaline medium was studied and compared among the catalysts.

2. Experimental

2.1. Preparation of Pd/CNTs, Pd/XC-72 and Pd/GNPs catalysts

Catalysts were prepared through microwave-assisted EGreduction with Pd loading of 20 wt%. For the synthesis of Pd/CNTs, 120 mg of CNTs were placed in a three-necked flask containing 20 mL of EG and mixed well.Under ultrasonic dispersion for 15 min, 12.7 mL of 2.36 mg/mL $PdCl_2$EG solution was added. pH value was adjusted by adding NaOH (0.1 M) solution to 12, and ultrasonic dispersion was continued for another 15 min. The mixture was then placed in an oil bath, heated at 130 °C for 2 h under magnetic stirring, allowed to stand and then filtered.The filtratewas washed with deionised water until complete Cl- removal and fully dried to prepare a Pd/CNT catalyst. Pd/XC-72 and Pd/GNP catalysts were prepared using the same steps as Pd/CNTs, except for the use of 120 mg of graphene nanosheets or 120 mg of XC-72 (XC-72)as replacement for 120 mg of CNTs.

2.2. Preparation of Pd/mix support catalysts

Catalyst hybrid supports (CNTs-GNPs, CNTs-XC-72 and XC-72-GNPs) were prepared as follows. The mixed sample CNTs-GNPs were ground for approximately 20 min, added with 30 mL of EG, ultrasonically dispersed for 15 min, added with 12.7 mL of 2.36 mg/mL $PdCl_2$EG solution, and ultrasonically dispersed again for 15 min. The pH of the above mixture was adjusted to 12 with NaOH EG solution, and ultrasonic dispersion was continued for another 15 min. The mixture was then placed in an oil bath, heated at 130 °C for 2 h under magnetic stirring, cooled and filtered at room temperature. The filtrate was washed with deionised water until complete Cl^- removal and dried sufficiently to prepare Pd/CNTs-GNPs catalysts. All the catalysts were prepared with the mass ratios of 1:0.5, 1:0.2, 1:0.1 and 1:0.06.

Other mixed supports including Pd/CNTs-XC-72 and Pd/XC-72-GNPs were prepared using the previous method for the catalysts.

2.3. Characterisation

TEM images were obtained employing a JEOL JEM-2000 EX microscope at 120 kV. X-ray diffraction (XRD) patterns were acquiredat tube voltage ~40 kV, tube current ~30 mA and scanning rate ~5°/min. Thermo VG ESCALAB250 multifunction surface analysis system was used to measure X-ray photoelectron spectra (XPS). At 284.6 eV, C1s level was used to correct the collected XPS spectra.

2.4. Electrode preparation

For the preparation of catalyst ink, 5 mg of the catalyst was added to 25 μL of Nafion solution and 1 mL of ethanol and ultrasonically dispersed for 15 min. A glassy carbon electrode (GCE) with diameter of 4 mm was rinsed with ethanol and deionised water and dried at room temperature. A micro-injector was used to drop 25 μL of the slurry onto the surface of GCE, which was then dried for later use as a working electrode.

Electrochemical tests, namely, CV, LSV, CA and EIS were carried out in a three-electrode single-compartment Pyrex glass cell. A GCE (4 mm) was used as a working electrode, and a Pt electrode 213 and Hg/HgO were applied as auxiliary and reference electrodes, respectively.The scanning range of the CV curve was

between −1 and 0.2 V, and the catalyst was activated by scanning the CV potential at a scanning rate of 50 mV/s. When the CV curve reached stability, the scan rate was changed to 20 mV/s, and the test was performed again. The remaining electrochemical tests (LSV, CA and EIS) were carried out after the completion of the CV test. All electrochemical experiments with and without containing methanol were performed in 0.5 mol/L KOH and 1.0 mol/L CH_3OH. The electrochemical performances of catalysts were investigated using a GAMRY Reference 3000 potentiostat/galvanostat. Prior to testing, the solution was deaerated with high-purity nitrogen. All experiments were carried out at 25 °C.

3. Results and discussion

3.1. Physical characterisation

3.1.1. TEm

Fig. 1 shows the TEM images of catalysts. In Pd/CNTs (Fig. 1a), the metal particles supported by CNTs are locally agglomerated. In the Pd/XC-72catalyst (Fig. 1b), the dispersion of Pd nanoparticles is poor, and the particles have agglomerated. In the Pd/GNPs catalyst (Fig. 1c), the distribution of Pd nanoparticles is extremely uneven, and the majority of the surface is not supported by metal particles. Some degree of Pd-nanoparticles aggregation can be noted. In the Pd/CNTs-GNPs catalyst (Fig. 1d), Pd particles are evenly distributed on the CNTs and graphene nanosheets, and almost no local agglomeration can be observed. In the Pd/CNTs-XC-72 catalyst (Fig. 1e), the distribution of Pd particles is relatively uniform without local agglomeration. In the Pd/XC-72-GNPs catalyst (Fig. 1f), the Pd nanoparticles have a small particle size and a uniform distribution.Therefore, the use of mixed carriers can effectively inhibit the occurrence of agglomeration to uniformly distribute and fix the metal components of the catalyst on the surface of the hybrid carbon support.

3.1.2. XRd

Fig. 2 shows the XRD patterns of prepared catalysts. For all catalysts, the diffraction peaks at 2θ diffraction angles of 40.0°, 46.4°, 68.0° and 81.9° correspond to the (111), (200), (220) and (311) lattices of the Pd face-centred cubic crystal structure, respectively.The Pd (220) peak at the 2q angle of 67.8° was chosen for the estimationof catalyst particle size with Scherrer's equation. The results show that the average particle diameters of Pd/CNTs, Pd/XC-72 and Pd/GNPs are 4.54,5.15 and 5.89 nm, respectively [Fig. 2(a, b and c)], and those of Pd/CNTs-GNPs, Pd/CNTs-XC-72, Pd/XC-72-GNPs are 4.51, 4.35 and 4.04 nm, respectively.

Compared with the single supports, the Pd/CNT-GNP catalysthas widerPd diffraction peak and smaller average particle size,

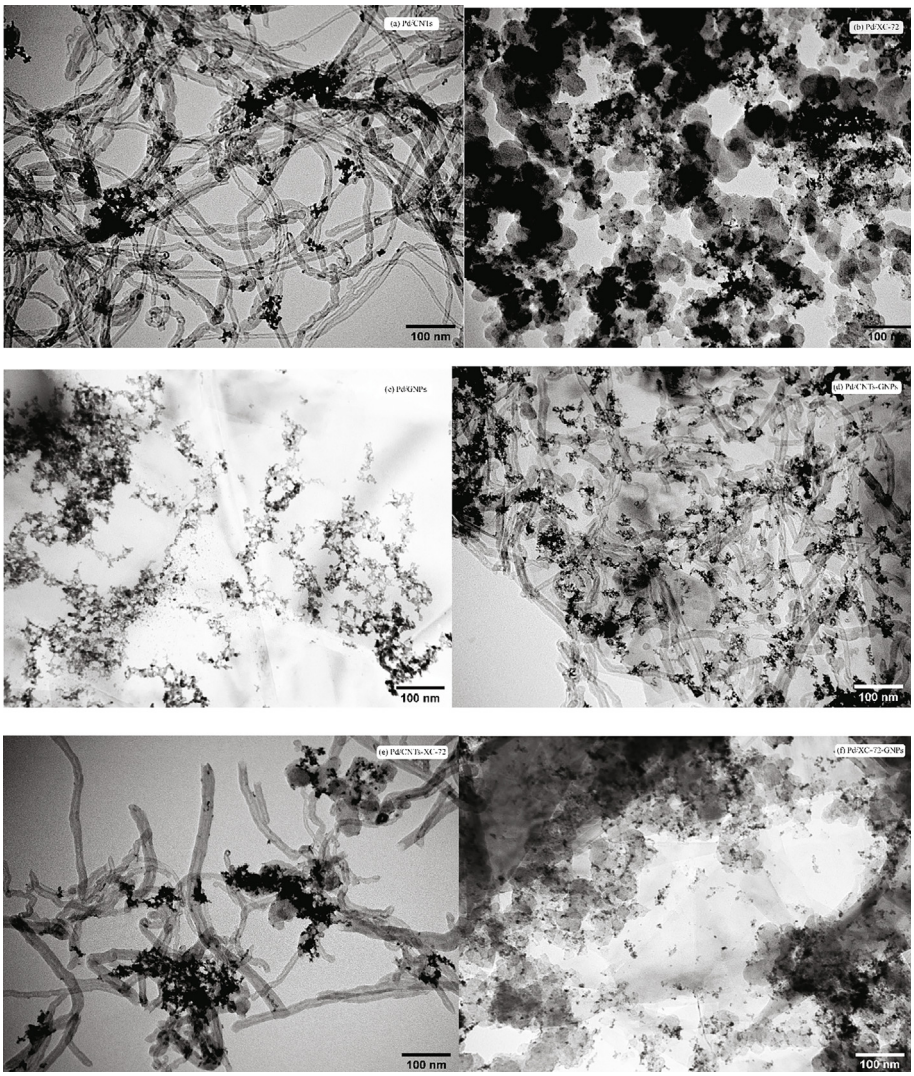

Fig. 1. TEM photographs of catalysts (a) Pd/CNTs, (b) Pd/XC-72, (c) Pd/GNPs, (d) Pd/CNTs-GNPs, (e)Pd/CNTs-XC-72 and (f) Pd/XC-72-GNPs.

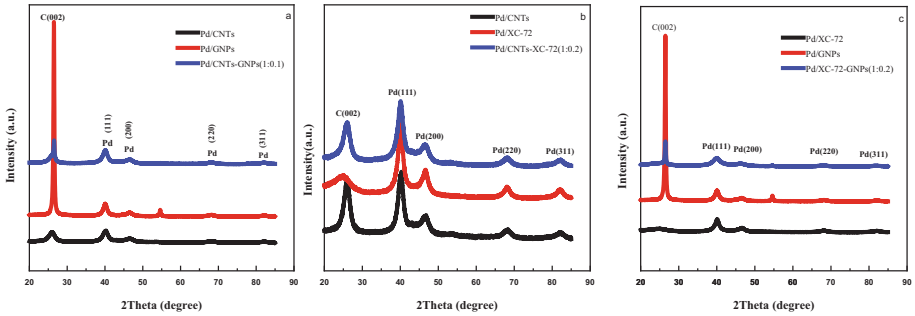

Fig. 2. X-ray diffractograms of the Pd/CNTs-GNPs, Pd/CNTs-XC-72 and Pd/XC-72-GNPs catalysts.

indicating the good dispersion effect of Pd nanoparticles on the CNTs-GNPs carrier. The diffraction peak at around 25° [Fig. 2(b)] is attributed to the carbon (002) crystal plane of the hexagonal graphite structure. Compared with that inthe highly graphitised CNTs, the carbon in XC-72 has an amorphous structure and thus has a wider (002) diffraction peak. Hence, the Pd/CNTs-GNPs catalyst has a wide Pd diffraction peak and small particles. The mixed carrier composed of CNTs and XC-72 has better dispersing ability for metal components than single supports. As shown in Fig. 2(c), the average particle size of Pd/XC-72-GNPs catalyst is only 4.04 nm, indicating that the large diffraction peak and small average particle size of this catalyst lead to a good dispersion effect. This finding is consistent with the TEM results.

3.1.3. XPs

Fig. 3$a_{1\text{-}3}$ shows the Pd 3d XPS spectra of Pd/CNTs, Pd/XC-72 and Pd/GNPs catalysts, and Fig. 3.$b_{1\text{-}3}$ shows the Pd 3d XPS spectra of Pd/CNTs-GNPs, Pd/CNTs-XC-72 and Pd/XC-72-GNPs catalysts. The XPS data of all catalysts are peak-fitted as shown in Table 1. All the catalysts have two peaks near the binding energies of 335.5 and 336.8 eV which correspond to Pd (0) and Pd (II), respectively. The contents of Pd (0) and Pd (II) varyin the three single-support catalysts.

The Pd (0) content of the three catalysts was compared.The results of the supported catalysts are consistent, that is, the Pd (0) content ofPd/CNTs-GNPs, Pd/CNTs-XC-72 and Pd/XC-72-GNPs catalysts are lower than those of Pd/CNTs, Pd/XC-72 and Pd/GNPs catalysts using mixed support. Therefore, the use of a mixed carrier can improve the structure of the catalyst and enhance the interaction between the metal components and the oxygen-containing functional groups on the surface of the mixed carrier. This finding can be attributed to the role of oxygen-containing functional groups on the surface of the mixed carrier. A strong interaction possibly occurs between the mixed carrier and the metal components and thus increases the oxidation state of Pd.

Table 1
The XPS data of Pd 3d in all catalysts.

Electrocatalysts	Binding energy / eV	Relative ratio / %
Pd/CNTs	335.5	68.8
	336.8	31.2
Pd/XC-72	335.5	69.4
	336.8	30.6
Pd/GNPs	335.5	71.4
	336.8	28.6
Pd/CNTs-GNPs	335.5	67.8
	336.8	32.2
Pd/CNTs-XC-72	335.5	67.9
	336.8	32.1
Pd/XC-72-GNPs	335.5	63.8
	336.8	36.2

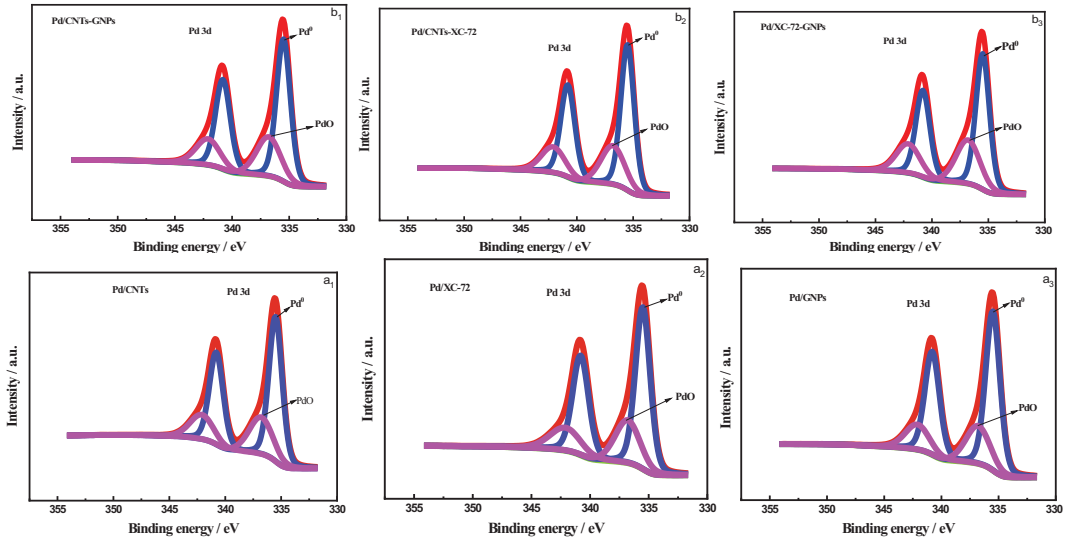

Fig. 3. XPS spectrum of Pd 3d in (a_1) Pd/CNTs, (a_2) Pd/XC-72, (a_3) Pd/GNPs, (b_1) Pd/CNTs-GNPs, (b_2) Pd/CNTs-XC-72 and (b_3) Pd/XC-72-GNPs catalysts.

3.2. Electrochemical performance

3.2.1. Cv

The CV of the Pd nanoparticles of all catalysts were recorded in the potential region from −1.0 V to +0.30 V at the scan rate of 50 mVs^{-1} in 0.5 mol/L KOH solution at 25C. As shown in Fig. 4.1(a), hydrogen adsorption peaksappear in the potential area of 1.00–0.60 V. The catalysts with mixed support all show clear hydrogen adsorption peaks, and their ECSA is remarkably larger than that of the catalyst with single support. In the figures, ECSA is represented by the Pd oxide reduction peak in the backward scan of the potential region from 0.10 V to 0.50 V (transformation of palladium metal into palladium (II) oxide).In Pd/CNTs-GNPs (1:0.1), Pd/CNTs-XC-72(1:0.2) and Pd/XC-72-GNPs (1:0.2), this areais significantly larger than that in Pd/CNTs, Pd/XC-72 and Pd/GNPs. This finding is ascribed to the unique structure of these hybrid supports that allow full surfaceutilisation.

Fig. 4.2(a) shows that theoxidation peak current densities of Pd/CNTs-GNPs (1:0.1), Pd/CNTs-GNPs (1:0.2), Pd/CNTs-GNPs (1:0.5) and Pd/CNTs-GNPs (1:0.06) are 57.34, 49.34, 41.49 and 33.77 mA/cm^2, respectively. All these values are greater than those of Pd/CNTs (28.45 mA/cm^2) and Pd/GNPs (24.80 mA/cm^2) catalysts. Among which, Pd/CNTs-GNPs (1:0.1) catalyst has the highest oxidation peak current density which is attributed to the increase in active sites on the catalyst surface. When mixed with the graphene nanosheets, the CNTs are either dispersed on the surface or filled in the gaps between the graphene nanosheets. The distance between the graphene nanosheets is increased, and Pd nanoparticles can be loaded on both sides of the graphene nanosheets. Therefore, the specific surface area of the graphene nanosheets and CNTs can be fully utilised to form a unique spatial structure of the hybrid carrier which increases the available surface area of the carbon support and is beneficial to the loading of Pd nanoparticles. Fig. 4.2(b) shows that the methanol oxidation peak current density of Pd/CNTs-XC-72 (1:0.2) catalyst is 50.88 mA/cm^2, which is significantly higher than those of Pd/CNTs (28.70 mA/cm^2) and Pd/XC-72 (30.68 mA/cm^2) catalysts. This finding can be attributed to the unique spatial structure of the mixed carrier composed of CNTs and XC-72 which facilitates the loading and dispersion of nanoparticles. Additionally, the oxygen-containing functional groups on the surface of the mixed carrier (ex: –OH and –COOH) increase the surface-active sites of the catalyst and improve its catalytic performance. Fig. 4.2(c) also shows that the methanol oxidation peak current densities of Pd/GNPs-XC-72 (1:0.2) catalyst is 37.74 mA/cm^2, which is higher than those of Pd/XC-72 and Pd/GNPs catalysts (30.75 and 24.76 mA/cm^2, respectively). After the graphene nanosheets are mixed with (XC-72), the structure is optimised which increases the carrier's usable surface area. This phenomenon is conducive to the loading of metal particles and increases the active sites on the catalyst surface, which in turn is conducive to the improvement of catalyst activity. Compared with that of single carbon support, the structure of mixed carbon support promotes the dispersion of Pd nanoparticles and provides thecatalyst with many active sites. This structure also effectively reduces the mass transfer resistance, thus allowing the reactants to easily approach the catalyst's active site. This result is in line with the ECSA findings.

3.2.2. LSv

Fig. 5(a, b and c) shows the LSV curves of mixed and single support catalysts towards methanol oxidation in 0.5 mol/L KOH and 1.0 mol/L CH_3OH solution. As shown in Fig. 5(a), the methanol oxidation onset potential of Pd/CNT-GNP (1:0.1) catalyst is −0.371 V, which is lower than those of Pd/CNTs and Pd/GNPs catalysts (−0.359 and −0.271 V, respectively).This finding indicates that the use of a mixed carrier composed of CNTs and graphene can reduce the methanol oxidation overpotential of the catalyst and improve its catalytic performance. As shown in Fig. 5(b), the initial oxidation potential of methanol on the Pd/CNT-XC-72 (1:0.2) catalyst is −0.591 V, and those of Pd/CNT and Pd/xc-72 catalysts are −0.485, and −0.404 V, respectively. Therefore, the use of mixed catalyst supports (CNTs and (XC-72)) can improve the kinetic performance and reduce the initial potential of the methanol electrooxidation reaction. Fig. 5(c) shows that the methanol

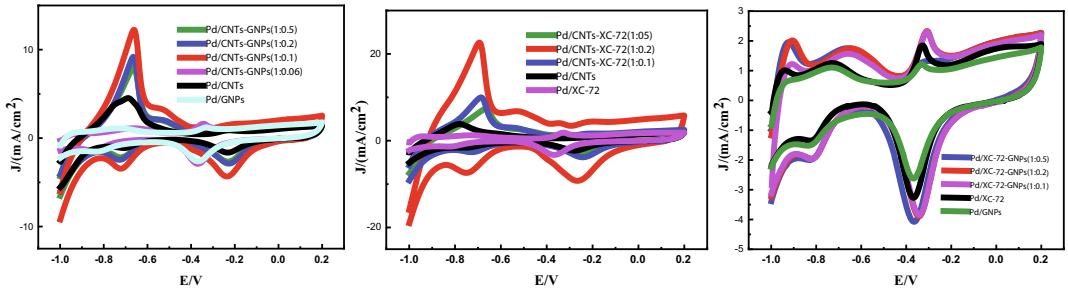

Fig. 4.1. (a) Shows CV curves of prepared catalysts in 0.5 mol/L KOH-1.0 mol/L.

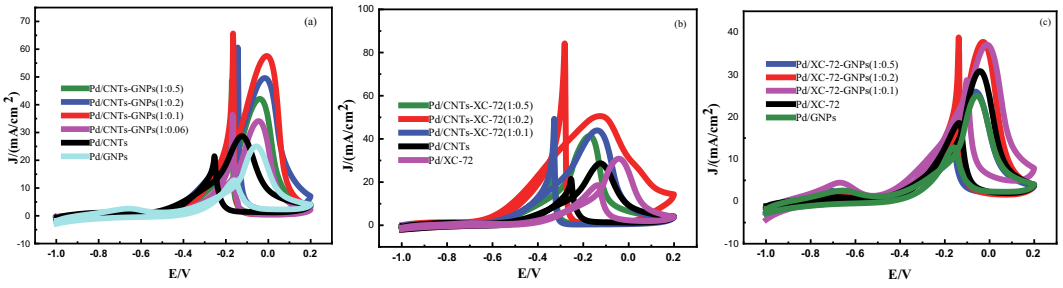

Fig. 4.2. (b) Cyclic voltammetry curves of all prepared catalysts in KOH (0.5 M)-CH_3OH (1.0 M) solution.

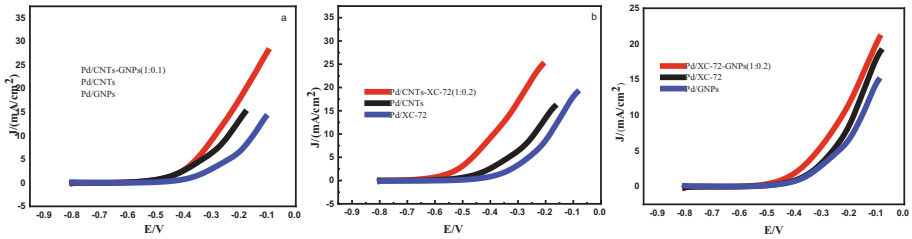

Fig. 5. Linear sweep voltammetry curves of prepared catalysts.

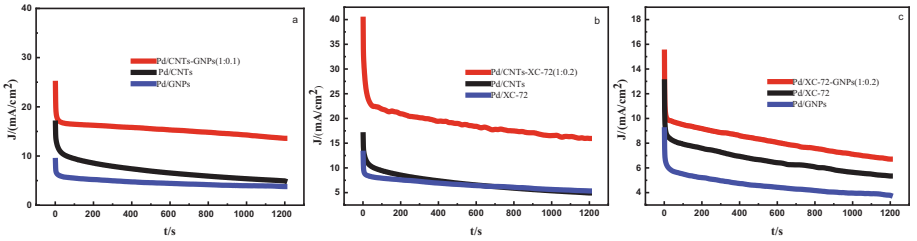

Fig. 6. Chronoamperometric curves of prepared catalysts.

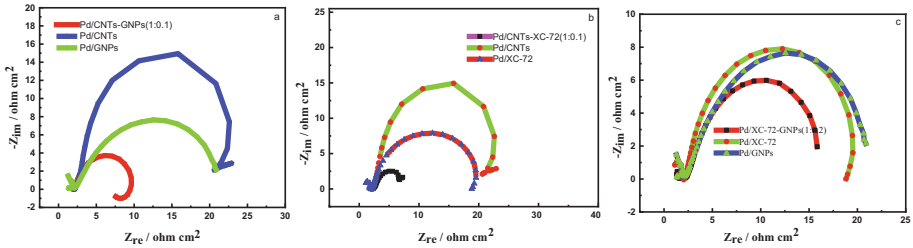

Fig. 7. Electrochemical impedance spectra ofprepared catalysts.

oxidation onset potential of Pd/XC-72-GNPs (1:0.2) catalyst (−0.507 V) is significantly lower than those of catalysts Pd/XC-72 (−0.463 V) and Pd/GNPs (−0.455 V). The negative shift of the initial potential of Pd/XC-72-GNPs (1:0.2) for methanol oxidation indicates that the use of mixed supports improves the kinetic performance of the catalyst and reduces the overpotential of the methanol electrooxidation reaction. This finding may be related to the change in the spatial structure of Pd/XC-72-GNPs (1:0.2) catalyst brought about by the mixed carrier.

3.2.3. Ca

The chronoamperograms of active catalysts Pd/CNTs-GNPs, Pd/CNTs-XC-72, and Pd/XC-72-GNPs were recorded at a potential of 0.50 V in 0.5 M KOH and 1 M CH_3OH solution to evaluate the poison resistance of catalysts towards methanol oxidationas shown in Fig. 6(a, b and c). During the entire test, the activity decay ratio or the performance degradation ratio of Pd/CNTs-GNPs (1:0.1), Pd/CNTs-XC-72 (1:0.2), and Pd/XC-72-GNPs (1:0.2) are 45%, 59% and 56% respectively, and the current density decay ratio of Pd/CNTs, Pd/XC-72 and Pd/GNP catalysts are 58%, 60%, and 70%, respectively. Therefore, the mixedsupport-based catalysts have higher stability and stronger poisoning resistanceto intermediate products than those with single support. This finding can be attributed to the unique spatial structure of the mixed carrier. After the CNTs are mixed with the graphene nanosheets, the available surface area increases, and the electrochemical stability of the catalyst is improved. Additionally, mixing (XC-72) with CNTs or with graphene nanosheets increases the available surface area of the carbon support and forms a unique spatial structure that enhances the anti-poisoning ability and electrochemical stability of the catalyst.The oxygen-containing functional groups on the surface also affect the stability of the catalysts.

3.2.4. EIs

Fig. 7 shows the EIS of Pd/CNTs-GNPs, Pd/CNTs-XC-72 and Pd/XC-72-GNPs versus Pd/CNTs, Pd/XC-72 and Pd/GNPs in alkaline methanol solution. The charge transfer resistance of Pd/CNTs-GNPs, Pd/CNTs-XC-72, and Pd/XC-72-GNPs is smaller than that of their components. Therefore, the mixing of CNTs with GNPs expedites methanolelectrooxidation [Fig. 7(a)]. This finding can also be explained by the structure of the mixed support composed of (XC-72) and CNTs. The mixing of carbon materials with different structures and scales increases the utilisation rate of the material surface and improves the mass transfer performance of reactants as shown in Fig. 7(b). Additionally, the (XC-72) and GNP nanosheets come in contact to form a carrier with a unique spatial structure which increases the active sites of the catalyst and the methanol electrooxidation rate on Pd/XC-72-GNPs (1:0.2) catalyst. As a result, the charge transfer resistance decreases. Therefore, the mixed support has a clear promoting effect on methanolelectrooxidation reaction as shown in Fig. 7(c).

4. Conclusions

Pd-based anodecatalysts (Pd/CNTs-GNPs, Pd/CNTs-XC-72 and Pd/XC-72-GNPs) for DMFCs were prepared throughEG reduction

by using a hybrid carbon carrier.Their catalytic performance towards methanol electrooxidation in an alkaline medium and their electrochemical stability were investigated. Compared with those using single carbon support, the catalysts based on hybrid supports (CNTs-GNPs, CNTs-XC-72 and XC-72-GNPs) showed higher catalytic activity in electrochemical tests, especially when the proportion of graphene nanosheets and (XC-72) in the mixed carriers was relatively small, such as in CNTs-GNPs (1:0.1), CNTs-XC-72 (1:0.2) and XC-72-GNPs (1:0.2). After the hybrid support was used, the content of Pd (0) species (in the form of metal) in the catalyst was reduced due to the interaction between Pd nanoparticles and the oxygen-containing functional groups on the carbon support. Comparison of the methanol electrooxidation performance among the three types of mixed carrier supported catalystsreveals that the Pd/CNTs-GNPs (1:0.1) catalysthas the highest methanol oxidation activity. This findingcan be attributed to the structural optimisation between CNTs and graphene nanosheets. CNTs effectively use the size advantage to increase the distance between graphene nanosheets, prevent them from agglomerating and significantly improve the dispersion performance of the carrier. Therefore, the use of a hybrid carbon carrier in the anode catalyst of DMFC is beneficial.

Declaration of Competing Interest

The authors declare that they have no known competing financial interests or personal relationships that could have appeared to influence the work reported in this paper.

Acknowledgements

This work was supported bythe National Natural Science Foundation of China (Grant No. 21273152) & The authors extend their appreciation to the Researchers Supporting Project number (RSP-2021/396), King Saud University, Riyadh, Saudi Arabia.

References

Al-Zaqri, N., Pooventhiran, T., Alsalme, A., Warad, I., John, A.M., Thomas, R., 2020. Structural and physico-chemical evaluation of melatonin and its solution-state excited properties, with emphasis on its binding with novel coronavirus proteins. J. Mol. Liq. 318, 114082.

Badran, I., Tighadouini, S., Radi, S., Zarrouk, A., Warad, I., 2021. Experimental and first-principles study of a new hydrazine derivative for DSSC applications. J. Mol. Struct. 1229, 129799.

Calderón Gómez, J.C., Moliner, R., Lázaro, M.J., 2016. Palladium-based catalysts as electrodes for direct methanol fuel cells: a last ten years review. Catalysts 6, 130.

Cao, E., Chen, Z., Wu, H., Yu, P., Wang, Y., Xiao, F., Chen, S., Du, S., Xie, Y., Wu, Y., Ren, Z., 2020. Boron-induced electronic-structure reformation of CoP nanoparticles drives enhanced pH-universal hydrogen evolution. Angew. Chem., Int. Ed. 59 (10), 4154–4160.

Carvalho, L.L., Colmati, F., Tanaka, A.A., 2017. Nickel–palladium electrocatalysts for methanol, ethanol, and glycerol oxidation reactions. Int. J. Hydrogen Energy 42 (25), 16118–16126.

Chen, W., Zhu, Z., Al-Khawlani, A., Yuan, Q., 2020. A Pd nanocatalyst supported on a polymer-modified hybrid carbon material for methanol oxidation. J. Appl. Electrochem. 50 (10), 1059–1067.

Chen, W., Zhu, Z., Yang, L., 2017. Palladium nanoparticles supported on a chitosan-functionalized hybrid carbon material for ethanol electro-oxidation. Int. J. Hydrogen Energy 42 (38), 24404–24411.

Chiang, Y.-C., Ciou, J.-R., 2011. Effects of surface chemical states of carbon nanotubes supported Pt nanoparticles on performance of proton exchange membrane fuel cells. Int. J. Hydrogen Energy 36 (11), 6826–6831.

Çögenli, M.S., Yurtcan, A.B., 2019. Carbon-based nanomaterials for alcohol oxidation. Nanomater. Alcohol Fuel Cells 49, 1–78.

Daş, E., Kaplan, B.Y., Gürsel, S.A., Yurtcan, A.B., 2019. Graphene nanoplatelets-carbon black hybrids as an efficient catalyst support for Pt nanoparticles for polymer electrolyte membrane fuel cells. Renew. Energy 139, 1099–1110.

Fan, Y., Zhao, Y., Chen, D., Wang, X., Peng, X., Tian, J., 2015. Synthesis of Pd nanoparticles supported on PDDA functionalized graphene for ethanol electro-oxidation. Int. J. Hydrogen Energy 40 (1), 322–329.

Fu, K., Wang, Y., Mao, L., Yang, X., Jin, J., Yang, S., Li, G., 2018. Facile morphology controllable synthesis of PtPd nanorods on graphene-multiwalled carbon nanotube hybrid support as efficient electrocatalysts for oxygen reduction reaction. Mater. Res. Bull. 108, 187–194.

Garba, Z.N., Zhou, W., Zhang, M., Yuan, Z., 2020. A review on the preparation, characterization and potential application of perovskites as adsorbents for wastewater treatment. Chemosphere 244.

Gharibi, H., Javaheri, M., Mirzaie, R.A., 2010. The synergy between multi-wall carbon nanotubes and Vulcan XC72R in microporous layers. Int. J. Hydrogen Energy 35 (17), 9241–9251.

Ghosh, A., Basu, S., Verma, A., 2013. Graphene and functionalized graphene supported platinum catalyst for PEMFC. Fuel Cells 13 (3), 355–363.

Li, Y., Li, Y., Zhu, E., McLouth, T., Chiu, C.-Y., Huang, X., Huang, Y.u., 2012. Stabilization of high-performance oxygen reduction reaction Pt electrocatalyst supported on reduced graphene oxide/carbon black composite. J. Am. Chem. Soc. 134 (30), 12326–12329.

Liu, M., Zhang, R., Chen, W., 2014. Graphene-supported nanoelectrocatalysts for fuel cells: synthesis, properties, and applications. Chem. Rev. 114 (10), 5117–5160.

Liu, Z., Abdelhafiz, A.A., Jiang, Y., Qu, C., Chang, I., Zeng, J., Liao, S., Alamgir, F.M., 2019. Pt/graphene with intercalated carbon nanotube spacers introduced by electrostatic self-assembly for fuel cells. Mater. Chem. Phys. 225, 371–378.

Lv, Y., Wu, X., Lin, H.e., Li, J., Zhang, H., Guo, J., Jia, D., Zhang, H., 2021. A novel carbon support: few-layered graphdiyne-decorated carbon nanotubes capture metal clusters as effective metal-supported catalysts. Small 17 (12), 2006442.

Mu, X., Xu, Z., Ma, Y., Xie, Y., Mi, H., Ma, J., 2017. Graphene-carbon nanofiber hybrid supported Pt nanoparticles with enhanced catalytic performance for methanol oxidation and oxygen reduction. Electrochim. Acta 253, 171–177.

Nguyen, S.T., Ling Tan, D.S., Lee, J.-M., Chan, S.H., Wang, J.Y., Wang, X., 2011. Tb promoted Pd/C catalysts for the electrooxidation of ethanol in alkaline media. Int. J. Hydrogen Energy 36 (16), 9645–9652.

Ning, L., Liu, X., Deng, M., Huang, Z., Zhu, A., Zhang, Q., Liu, Q., 2019. Palladium-based nanocatalysts anchored on CNT with high activity and durability for ethanol electro-oxidation. Electrochim. Acta 297, 206–214.

Pham, K.-C., McPhail, D.S., Mattevi, C., Wee, A.T.S., Chua, D.H.C., 2016. Graphene-carbon nanotube hybrids as robust catalyst supports in proton exchange membrane fuel cells. J. Electrochem. Soc. 163 (3), F255.

Saleemh, F.A., Musameh, S., Sawafta, A., Brandao, P., Tavares, C.J., Ferdov, S., Barakat, A., Al Ali, A., Al-Noaimi, M., Warad, I., 2017. Diethylenetriamine/diamines/copper (II) complexes [Cu (dien)(NN)] Br 2: Synthesis, solvatochromism, thermal, electrochemistry, single crystal, Hirshfeld surface analysis and antibacterial activity. Arab. J. Chem. 10, 845–854.

Schulze, M.C., Belson, R.M., Kraynak, L.A., Prieto, A.L., 2020. Electrodeposition of Sb/CNT composite films as anodes for Li-and Na-ion batteries. Energy Storage Mater. 25, 572–584.

Shao, M., 2011. Palladium-based electrocatalysts for hydrogen oxidation and oxygen reduction reactions. J. Power Sources 196 (5), 2433–2444.

Staykov, A., Ooishi, Y., Ishihara, T., 2014. Immobilizing metal nanoparticles on single wall nanotubes. Effect of surface curvature. J. Phys. Chem. C 118 (17), 8907–8916.

Suzuki, T., Hashizume, R., Hayase, M., 2015. Effect of blending carbon nanoparticles and nanotubes on the formation of porous structure and the performance of proton exchange membrane fuel cell catalyst layers. J. Power Sources 286, 109–117.

Tang, X., Zeng, Y., Cao, L., Yang, L., Wang, Z., Fang, D., Gao, Y., Shao, Z., Yi, B., 2018. Anchoring ultrafine Pt nanoparticles on the 3D hierarchical self-assembly of graphene/functionalized carbon black as a highly efficient oxygen reduction catalyst for PEMFCs. J. Mater. Chem. A 6 (31), 15074–15082.

Wang, Y.-J., Fang, B., Li, H., Bi, X.T., Wang, H., 2016. Progress in modified carbon support materials for Pt and Pt-alloy cathode catalysts in polymer electrolyte membrane fuel cells. Prog. Mater. Sci. 82, 445–498.

Warad, I., Eftaiha, A. a F., Al-Nuri, M.A., Husein, A.I., Assal, M., Abu-Obaid, A., Al-Zaqri, N., Hadda, T. Ben, Hammouti, B., 2013. Metal ions as antitumor complexes-Review. J. Mater. Environ. Sci 4, 542–557.

Warad, I., Khan, A.A., Azam, M., Al-Resayes, S.I., Haddad, S.F., 2014. Design and structural studies of diimine/CdX2 (X= Cl, I) complexes based on 2, 2-dimethyl-1, 3-diaminopropane ligand. J. Mol. Struct. 1062, 167–173.

Wei, Y.-C., Liu, C.-W., Wang, K.-W., 2011. Improvement of oxygen reduction reaction and methanol tolerance characteristics for PdCo electrocatalysts by Au alloying and CO treatment. Chem. Commun. 47, 11927–11929.

Wu, B., Kuang, Y., Zhang, X., Chen, J., 2011. Noble metal nanoparticles/carbon nanotubes nanohybrids: synthesis and applications. Nano Today 6 (1), 75–90.

Yousaf, A.B., Imran, M., Zaidi, S.J., Kasak, P., 2019. Engineering and understanding of synergistic effects in the interfaces of rGO-CNTs/PtPd nanocomposite revealed fast electro-oxidation of methanol. J. Electroanal. Chem. 832, 343–352.

Zhang, M., Chen, J., Li, H., Cai, P., Li, Y., Wen, Z., 2019. Ru-RuO2/CNT hybrids as high-activity pH-universal electrocatalysts for water splitting within 0.73 V in an asymmetric-electrolyte electrolyzer. Nano Energy 61, 576–583.

Zhang, X., Zhang, J.-W., Xiang, P.-H., Qiao, J., 2018. Fabrication of graphene-fullerene hybrid by self-assembly and its application as support material for methanol electrocatalytic oxidation reaction. Appl. Surf. Sci. 440, 477–483.

Zhang, X., Zhang, X., Xu, H., Wu, Z., Wang, H., Liang, Y., 2017. Iron-doped cobalt monophosphide nanosheet/carbon nanotube hybrids as active and stable electrocatalysts for water splitting. Adv. Funct. Mater. 27 (24), 1606635.

Zhou, F., Sa, R., Zhang, X., Zhang, S., Wen, Z., Wang, R., 2020. Robust ruthenium diphosphide nanoparticles for pH-universal hydrogen evolution reaction with platinum-like activity. Appl. Catal. B Environ. 274.